

# SCIENTIFIC REPORTS



OPEN

## Glass transition of aqueous solutions involving annealing-induced ice recrystallization resolves liquid-liquid transition puzzle of water

Received: 15 June 2015  
Accepted: 28 September 2015  
Published: 27 October 2015

Li-Shan Zhao<sup>1,2</sup>, Ze-Xian Cao<sup>1</sup> & Qiang Wang<sup>1</sup>

Liquid-liquid transition of water is an important concept in condensed-matter physics. Recently, it was claimed to have been confirmed in aqueous solutions based on annealing-induced upshift of glass-liquid transition temperature,  $T_g$ . Here we report a universal water-content,  $X_{\text{aqu}}$ , dependence of  $T_g$  for aqueous solutions. Solutions with  $X_{\text{aqu}} > X_{\text{aqu}}^{\text{cr}}$  vitrify/devitrify at a constant temperature,  $-T_g'$ , referring to freeze-concentrated phase with  $X'_{\text{aqu}}$  left behind ice crystallization. Those solutions with  $X'_{\text{aqu}} < X_{\text{aqu}} < X_{\text{aqu}}^{\text{cr}}$  totally vitrify at  $T_g < T_g'$  under conventional cooling/heating process though,  $T_g$  of the samples annealed at temperatures  $> T_g$  to effectively evoke ice recrystallization is stabilized at  $-T_g'$ . Experiments on aqueous glycerol and 1,2,4-butanetriol solutions in literature were repeated, and the same samples subject to other annealing treatments equally reproduce the result. The upshift of  $T_g$  by annealing is attributable to freeze-concentrated phase of solutions instead of 'liquid II phase of water'. Our work also provides a reliable method to determine hydration formula and to scrutinize solute-solvent interaction in solution.

The first-order liquid-liquid transition (LLT), a hot topic of condensed matter physics and materials science per se, has drawn much attention particularly from researchers in water science since 1992<sup>1</sup>. Simulations suggested that supercooled water, depending on temperature and pressure, can exist in two distinct forms, namely, the low-density liquid water and the high-density liquid water<sup>2-5</sup>. The first-order phase transition between the low-density and high-density phases of water is speculated to terminate at a liquid-liquid critical point (LLCP) on the phase diagram<sup>1,6-11</sup>. Despite vehement debate<sup>12,13</sup>, the LLCP hypothesis has since been taken as one main mechanism responsible for various anomalous properties of supercooled water<sup>8,9,13-15</sup>. Regrettably, LLCP is believed to lie at a temperature lower than the homogeneous nucleation temperature of ice (235 K), which is thus inaccessible for supercooled bulk water<sup>16</sup>. Consequently, it is very difficult to verify experimentally the existence of the speculated liquid-liquid transition or to investigate the properties of the so-called second critical point for supercooled bulk water. In order to circumvent this obstacle, water in aqueous solutions<sup>17-19</sup> or confined within nanometer-sized pores<sup>8,20,21</sup> comes into scope. In these two cases, ice nucleation can be effectively suppressed, and water therein can be easily supercooled down to temperatures even far below the anticipated LLCP.

Recently, it was reported that annealing-induced LLT has been observed in supercooled aqueous solutions of glycerol<sup>18</sup> and 1,2,4-butanetriol<sup>19</sup>. Those solutions in the concentrations concerned there can totally vitrify upon cooling at a moderate rate, and the corresponding glass-liquid transition, i.e., the

<sup>1</sup>Beijing National Laboratory for Condensed Matter Physics, Institute of Physics, Chinese Academy of Sciences, Beijing 100190, China. <sup>2</sup>Department of Physics, University of Science and Technology Beijing, Beijing 100083, China. Correspondence and requests for materials should be addressed to Q.W. (email: qwang@aphy.iphy.ac.cn)

devitrification process, begins to appear on the heating curve at a temperature  $T_{gl}$ . This glass-liquid transition temperature was found to shift from  $T_{gl}$  to a higher value  $T_{gII}$  in a sample which has experienced annealing treatment, in the heating process, at a temperature  $T_a (> T_{gl})$  for a sufficiently long time. Besides glass transition temperature,  $T_g$ , other physical properties such as the fragility, density, temperature-dependent dielectric relaxation, and hydrogen bonding state all manifest obvious difference between the precursor and the annealed samples. These annealing-induced changes in glass-transition related properties are interpreted as evidence of liquid water polymorphism in the measured aqueous solutions. The conceived liquid phases of water in the precursor and annealed solutions are termed liquid I and liquid II phase of water, respectively, in the literature. However, as also noticed by the authors of refs.18 and 19, such an LLT of water is always accompanied by recrystallization of ice (in the heating process at a temperature higher than the glass-liquid transition temperature). To exclude the possibility that the claimed LLT of water is per facta due to ice recrystallization-induced macroscopic phase separation, time-dependent Raman spectra were measured to trace the change in hydrogen bonding state of the sample in the course of annealing treatment. A transition from high density amorphous water-like profile to low density amorphous water-like profile is claimed to be observed, and being consequently regarded as a circumstantial evidence of LLT.

In the current work, we report systematic measurement of the water-content dependence of glass transition temperature for various aqueous solutions in an as wide as possible range of concentration, which reveals a universal behavior that can set criteria to divide the solutions into three distinct zones. We noticed that for the medium-concentration aqueous solutions, glass-liquid transition can be complicated by ice recrystallization in the heating process depending on the thermal history, and the liquid phase II actually corresponds to the freeze-concentrated phase, i.e., the portion of the solution of an elevated but definite concentration resulting from water freezing, of the annealed solutions. We repeated the annealing treatments on the same solutions as reported in refs 18,19, and reproduced the result therein, which fits well with the data for freeze-concentrated phase which can be accessed simply upon cooling in water-rich solutions and accessed via designed annealing treatment in the medium-concentration solutions. Such a glass transition behavior related to the 'liquid II phase of water' can be reproduced in most electrolytic and organic solutions so long as they fall within the medium-concentration zone and a proper annealing treatment is applied. Together with the comparative study by using dielectric loss spectroscopy and Raman spectroscopy on solutions in the full concentration range available, it is concluded that the 'liquid II phase of water' refers to the freeze-concentrated phase prepared by annealing, and the claimed LLT for water in aqueous solutions based on glass transition temperature shift seems untenable. The universal water-content dependence of glass transition temperature is of essential importance in its own right.

## Results

**Universal water-content dependence of  $T_g$ .** The water-content dependence of  $T_g$  was measured for the aqueous solutions of glycerol, 1,2,4-butanetriol and  $AlCl_3$ , which manifests a quite universal feature (Fig. 1) when a conventional one-round cooling/heating process at a moderate rate ( $\leq 20$  K/min.) was adopted (for the typical DSC thermograms of solutions with different water contents, see Supplementary Fig. 1). The universal water-content dependence of  $T_g$  can also be verified in other solutions of electrolytes and organic substances, and their mixtures (see Supplementary Fig. 2. Measurements on more than 20 different solutions will be published elsewhere). Remarkably, for a given solute, the solutions of variable water content, or correspondingly concentration, can be divided into three distinct zones following the behavior of glass transition.

In Fig. 1a,  $T_g$  for the aqueous glycerol solutions, with increasing water content, first drops monotonically. The corresponding solutions with a mass fraction of water,  $X_{aqu}$ , below a critical value, i.e.,  $X_{aqu} < X_{aqu}^{cr}$ , can totally vitrify in the cooling process (see Supplementary Fig. 1b,c). This monotonous drop of  $T_g$  value with increasing water content results from the plasticizer effect of water. In contrast, in those solutions with  $X_{aqu} > X_{aqu}^{cr}$ , precipitation of primary ice occurs at first in the cooling process (a pronounced endothermic peak appears prior to the glass transition on DSC curve, see Supplementary Fig. 1a), thus glass-liquid transition temperatures stabilized at a constant value,  $T_g'$ , were measured, which arises from the devitrification of the freeze-concentrated phase. The water content for the freeze-concentrated phase,  $X'_{aqu}$ , which corresponds to the hydration formula for the given solute, can be directly read from the monotonous part of the  $T_g$  vs.  $X_{aqu}$  curve at the point where  $T_g = T_g'$ . With  $X'_{aqu}$  and  $X_{aqu}^{cr}$  at hand, the aqueous solutions can be divided into three distinct zones, marked as I, II, III in Fig. 1a, with regard to the glass transition behavior. For aqueous glycerol solution,  $T_g' = \sim 170$  K,  $X_{aqu}^{cr} = 0.526$ , and  $X'_{aqu} = 0.227$ . Since the freeze-concentrated phase of the water-rich solutions has a nearly constant concentration, it leads to a linear relationship between  $X_{aqu}$ , or the amount of freeze-concentrated phase, and the heat flow change per unit mass of solution at  $T_g$ , denoted as  $\delta_{Tg}$  (Fig. 1b). Reasonably, the linear dependence of  $\delta_{Tg}$  upon  $X_{aqu}$  can extend into zone II so long as ice precipitation has been successfully evoked prior to glass transition via a proper cooling/heating

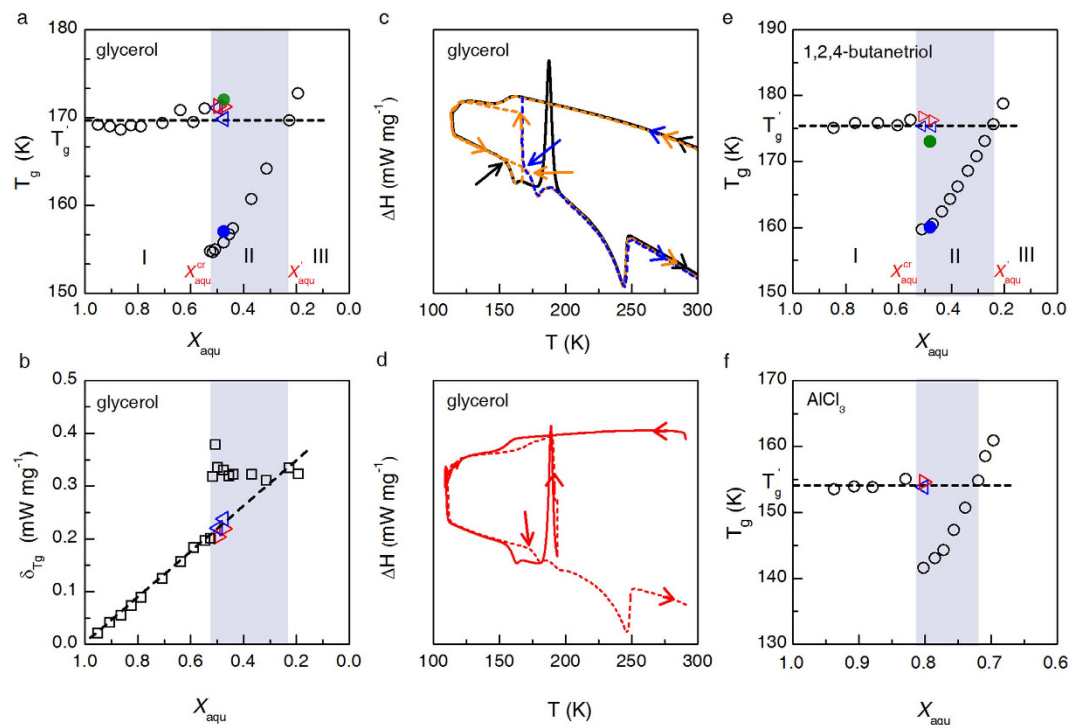


**Figure 1. Glass transition of aqueous solutions complicated by annealing-induced ice recrystallization.**

(a) Glass transition temperature,  $T_g$ , against the mass fraction of water,  $X_{\text{aqu}}$ , for glycerol solutions (empty circle) obtained under conventional cooling/heating process. In those solutions with a  $X_{\text{aqu}} > X_{\text{aqu}}^{\text{cr}}$ , ice precipitation occurs first in cooling process. The freeze-concentrated phases vitrify at a constant  $T_g'$ , and the corresponding  $X'_{\text{aqu}}$  can be directly read from the monotonous part of the  $T_g$  vs.  $X_{\text{aqu}}$  curve at the point where  $T_g = T_g'$ . Here  $T_g' = 170$  K,  $X_{\text{aqu}}^{\text{cr}} = 0.526$ ,  $X'_{\text{aqu}} = 0.227$ . For comparison,  $T_g$  data for the liquid I (blue solid circle) and liquid II (olive solid circle) phases of water in glycerol solution with  $X_{\text{aqu}} = 0.474$  reported in ref. 18 are presented. (b) Solution mass-normalized heat flow change at glass transition,  $\delta_{T_g}$ , as a function of  $X_{\text{aqu}}$  for glycerol solutions. The blue and red hollow triangles in (a,b) denote the data points for freeze-concentrated phases of glycerol solutions with  $X_{\text{aqu}} = 0.497$  and  $X_{\text{aqu}} = 0.474$  subjected to temperature protocol 2 and protocol 4 (see below), respectively. (c) DSC thermograms for three distinct temperature protocols demonstrated with the glycerol solution of  $X_{\text{aqu}} = 0.474$ . Protocol 1 (black line): Conventional cooling/heating process; protocol 2 (blue line): The cooling process is terminated at 167 K and maintained there for 230 min., followed by heating to room temperature; protocol 3 (orange line): The heating process is interrupted at 167 K and maintained there for 230 min. After that the sample was again cooled down to 113 K and then heated to room temperature. (d) Protocol 4: The heating process is interrupted at 194 K. After maintained there for 1 min. to complete ice recrystallization, the sample was again cooled down to 113 K and then heated to room temperature. Arrows pointing at the curves indicate where  $T_g$  is extracted. (e,f)  $T_g$  versus  $X_{\text{aqu}}$  for aqueous solutions of 1,2,4-butanetriol and  $\text{AlCl}_3$ , respectively. For the former,  $T_g' = 175$  K,  $X_{\text{aqu}}^{\text{cr}} = 0.531$ ,  $X'_{\text{aqu}} = 0.238$ ; for the latter,  $T_g' = 154$  K,  $X_{\text{aqu}}^{\text{cr}} = 0.812$ ,  $X'_{\text{aqu}} = 0.719$ . Again, the blue (protocol 2) and red (protocol 4) triangles corresponding to measurements with annealing treatment, and data from ref. 19 (solid circles), are presented.

procedure, as demonstrated by experiment on glycerol solutions with  $X_{\text{aqu}} = 0.497$  and  $X_{\text{aqu}} = 0.474$  subjected to cooling/heating procedures specified in protocol 2 (Fig. 1c) and protocol 4 (Fig. 1d). This feature confirms the picture that after ice precipitation, only the freeze-concentrated phase is involved in the vitrification and devitrification processes for solutions with some excessive water, i.e.,  $X_{\text{aqu}} > X'_{\text{aqu}}$ .

For those solutions falling in zone II with  $X'_{\text{aqu}} < X_{\text{aqu}} < X_{\text{aqu}}^{\text{cr}}$ , which do contain more water than required for the hydration of the solute molecules or ions, recrystallization of excessive water may be suppressed or not depending on the cooling/heating procedure applied. In this case, glass transition can be complicated by annealing-induced recrystallization of water (Fig. 1a,e), that annealing treatment at a temperature  $T_a > T_g$  that effectively evokes ice recrystallization will result in measuring an upshifted  $T_g$  which corresponds to  $T_g'$  for the freeze-concentrated phase. This seems to be the culprit for the misconceived liquid-liquid transition of water in previous researches.

**Annealing-induced ice recrystallization and LLT.** In order to verify our judgment, measurement on the aqueous glycerol solution investigated in ref. 18 will be exactly reproduced, and the sample will also be subjected to particularly designed annealing treatment. For the sample concerned, it has a molar fraction of glycerol of 0.178 which corresponds to  $X_{\text{aqu}} = 0.474$ . It simply vitrifies completely upon cooling at a moderate rate of  $20 \text{ K min}^{-1}$ . In the subsequent heating process, the devitrification process starting at  $T_{\text{g}} = 155.8 \text{ K}$  is followed by ice recrystallization as revealed by a pronounced exothermal peak on the DSC heating curve with an onset temperature  $T_{\text{onset}} \sim 180 \text{ K}$  (black line in Fig. 1c). However, we call for attention to the fact that such ice recrystallization can be deliberately manipulated by designing proper cooling/heating processes, namely, (1) the cooling process is terminated at a temperature  $T_{\text{a}}$  ( $T_{\text{g}} < T_{\text{a}} < T_{\text{onset}}$ ), and maintained there for a sufficiently long time, e.g., for 230 min. at  $T_{\text{a}} = 167 \text{ K}$ , which is then followed by heating up to room temperature (protocol 2, blue dashed line in Fig. 1c). In the annealing process, both ice recrystallization and liquid-glass transition have finished; (2) the heating process starting from 113 K is interrupted at a temperature  $T_{\text{a}}$  ( $T_{\text{g}} < T_{\text{a}} < T_{\text{onset}}$ ) and maintained for a sufficiently long time, e.g., for 230 min. at  $T_{\text{a}} = 167 \text{ K}$ . After that, the sample was again cooled down to 113 K and then heated up to room temperature (protocol 3, orange dashed line in Fig. 1c). One sees that the glass-liquid transition temperature thus measured in the heating process shifts to a higher value, in fact corresponding to  $T_{\text{g}}'$  for the freeze-concentrated phase. In Fig. 1d, the sample was immediately cooled down to 113 K from 194 K, obviously ice recrystallization has been brought to the end, thus also a transition temperature  $T_{\text{g}}'$  was subsequently measured. It is noteworthy that even annealing at such a high temperature ( $> T_{\text{onset}}$ ) for sufficiently long time in the cooling process, ice recrystallization can be equally effectively evoked (see Supplementary Fig. 3).

With these different annealing treatments, the exothermal peak corresponding to ice recrystallization are absent on the DSC heating curve. However, the endothermic peak corresponding to the melting process of recrystallized ice at  $\sim 245 \text{ K}$  always makes its presence. Moreover, the position and area of this endothermic peak remain unchanged irrespective of the different thermal histories, as it corresponds to a complete ice recrystallization in the sample. Figure 1a,c clearly show that the residual glycerol solutions left behind ice recrystallization vitrify totally at  $\sim 170 \text{ K}$  that corresponds to  $T_{\text{g}}'$  of aqueous glycerol solutions (Fig. 1a). The low-temperature phase of the annealed aqueous glycerol solutions within Zone II, similar to those in zone I with  $X_{\text{aqu}} > X_{\text{aqu}}^{\text{cr}}$ , comprises a mixture of crystallized ice and vitrified freeze-concentrated phase of the same water content specified by  $X'_{\text{aqu}}$ , which corresponds to the hydration formula of glycerol·1.5H<sub>2</sub>O. Without contribution from the precipitated ice the  $\delta_{T_{\text{g}}}$  data points of the annealed samples with  $X_{\text{aqu}} = 0.497$  and  $X_{\text{aqu}} = 0.474$  do fall on the linear extension of  $\delta_{T_{\text{g}}}$  data for solutions in zone I (Fig. 1b).

We want here to emphasize that the values of  $T_{\text{g}}' \sim 170 \text{ K}$  for the freeze-concentrated phases formed through various annealing treatments (Fig. 1c,d) agree well with that for the suggested 'liquid II phase of water' in glycerol solution with  $X_{\text{aqu}} = 0.474$ <sup>18</sup>. Therefore, conclusion can be drawn that the observed change in glass-liquid transition temperature of supercooled glycerol solutions there arises from macroscopic phase separation evoked by annealing treatment, rather than from the claimed liquid-liquid phase transition.

This kind of annealing-induced ice recrystallization and macroscopic phase separation can be observed in aqueous solutions of other electrolytes and organic substances so long as the solution falls within the respective Zone II. Figure 1e,f show the corresponding results for aqueous solutions of 1,2,4-butanetriol and AlCl<sub>3</sub>,  $T_{\text{g}}' = 175 \text{ K}$ ,  $X_{\text{aqu}}^{\text{cr}} = 0.531$ , and  $X'_{\text{aqu}} = 0.238$  for 1,2,4-butanetriol, while  $T_{\text{g}}' = 154 \text{ K}$ ,  $X_{\text{aqu}}^{\text{cr}} = 0.812$ , and  $X'_{\text{aqu}} = 0.719$  for AlCl<sub>3</sub>. In Fig. 1e, the two data points that are used to justify the existence of 'liquid II phase of water' in ref. 19 are present, again the claimed glass transition temperature for the liquid II phase is roughly  $T_{\text{g}}'$  for freeze-concentrated phase. More examples are presented in Supplementary Fig. 2. For effectively inducing complete ice recrystallization, annealing temperature and time should be chosen with regard to the solute type and solution concentration. As seen from Supplementary Fig. 3a,b, for a lower  $T_{\text{a}}$  (relative to  $T_{\text{onset}}$  which rises with increasing concentration) a longer annealing time will be needed. For example, ice recrystallization in glycerol solution with  $X_{\text{aqu}} = 0.474$  can be achieved by annealing for 230 min. at 167 K, however, at 164 K this is not done even for 480 min. The degree of ice recrystallization and consequently the concentration of freeze-concentrated phase can be evaluated by the exact value of  $T_{\text{g}}'$  of freeze-concentrated solution and the area of the exothermal recrystallization peak (see Supplementary Fig. 3c). An incomplete ice recrystallization may imply a lowered  $T_{\text{g}}'$  for the freeze-concentrated phase. By the way, ice recrystallization can also be evoked in the cooling process at a temperature  $> T_{\text{onset}}$ , but generally speaking, it can be more easily evoked on the heating process because the previous vitrification/devitrification process can strongly promote ice recrystallization (see Supplementary Fig. 3d).

**Dielectric loss spectrometric measurement.** Besides glass transition temperature, the dielectric relaxation time versus temperature relationship for aqueous solutions of different concentrations subject to annealing treatment or not can also be applied to resolve the puzzle. Dielectric loss spectra are fitted

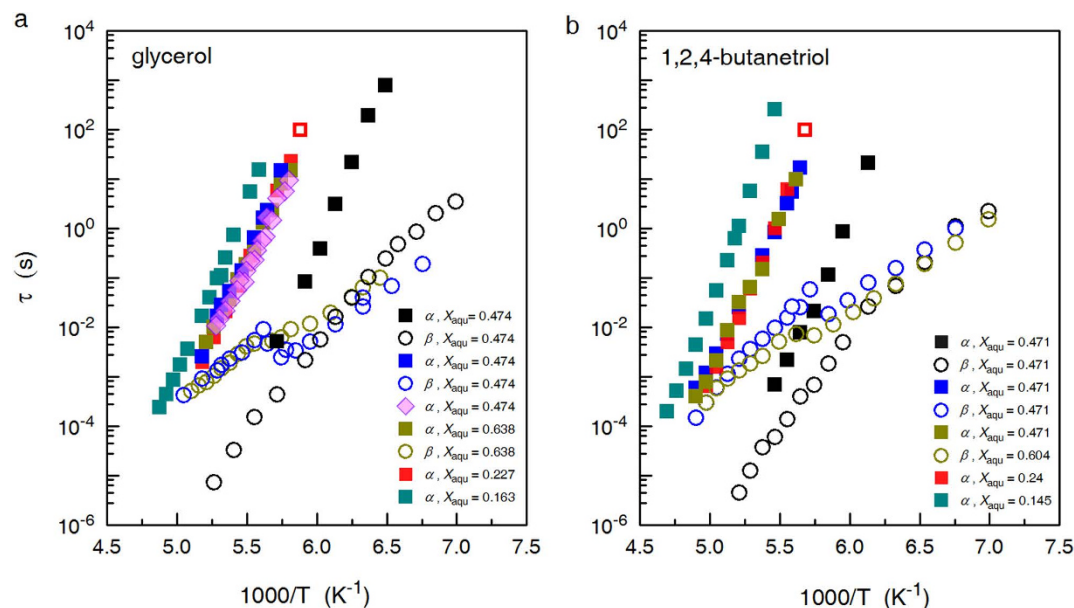


**Figure 2. Temperature-dependent relaxation times for aqueous solutions of glycerol and 1,2,4-butanetriol subject to different thermal histories.** (a) The relaxation times  $\tau_\alpha$  and  $\tau_\beta$  for aqueous glycerol solutions with  $X_{\text{aqu}}=0.638$  (I), 0.474(II), 0.227, and 0.163(III), respectively. Black symbols: the sample with  $X_{\text{aqu}}=0.474$  was cooled from room temperature down to each targeted temperature. After each measurement, the sample was then heated up to room temperature so as to avoid ice recrystallization and to ensure that the measured spectra correspond to a single supercooled liquid solution; Blue symbols: the cooling process was interrupted at 183 K where the sample was annealed for 150 min. After that, the sample was cooled down to 140 K, and then heated up to room temperature accompanied by spectral measurement; Magenta symbols:  $\tau_\alpha$  for glycerol solution with  $X_{\text{aqu}}=0.474$  reported as ‘liquid II phase of water’ in ref. 18; Dark yellow, red, and dark cyan symbols: the samples were heated from 140 K up to room temperature accompanied by spectral measurement; Red hollow square:  $\tau_\alpha$  (100s) for glycerol solution with  $X_{\text{aqu}} = 0.227$ . (b) Corresponding results for aqueous 1,2,4-butanetriol solutions. Blue symbols: the cooling process was interrupted at 195 K and maintained for 120 min. to ensure a complete ice recrystallization. After cooling down to 140 K, the sample was heating up to room temperature accompanied by spectral measurement. Other colored symbols denote the data points obtained following correspondingly the same procedure as in (a). For the two high-concentration samples in both cases, the  $\tau_\beta$  values are unavailable from fitting (see Supplementary Fig. 4).

according to Havriliak-Negami relaxation functions (for more details see Supplementary Fig. 4). The relaxation times  $\tau_\alpha$  and  $\tau_\beta$ , referring to the  $\alpha$  process and the Johari-Goldstein (or slow  $\beta$ ) process<sup>22</sup>, respectively, are plotted in Fig. 2 as a function of  $1000/T$ . For both glycerol and 1,2,4-butanetriol solutions, samples falling in all the three zones and that with  $X'_{\text{aqu}}$  are investigated, with the samples in zone (II) also subject to annealing treatment. Data from ref. 18 are included for comparison.

Obviously, the  $\tau_\alpha$  versus  $1000/T$  relationships are very similar for glycerol solutions with  $X_{\text{aqu}}=0.638$  (I),  $X'_{\text{aqu}}=0.227$ , and for the annealed sample with  $X_{\text{aqu}}=0.474$  (II).  $\tau_\alpha$  has been widely regarded to be related to the primary structural relaxation and glass transition<sup>23,24</sup>. The temperature where  $\tau_\alpha \sim 100$  s is very close to  $T_g$  determined on the basis of DSC measurement (see red hollow square in Fig. 2a). Therefore, it is reasonable to suggest that the  $\tau_\alpha$  versus  $1000/T$  relationship mainly reflects the structural relaxation of freeze-concentrated phase. That the concentrations of the freeze-concentrated phases in sample of zone I and in annealed sample of zone II are very close to  $X'_{\text{aqu}}=0.227$  results in a very similar temperature-dependence of  $\tau_\alpha$ . It comes as no surprise that the glycerol solution with  $X_{\text{aqu}}=0.474$  as claimed containing ‘liquid II phase of water’, displays a similar  $\tau_\alpha$  versus  $1000/T$  curve. Figure 2b tells the same story on the 1,2,4-butanetriol solutions, where the sample with  $X_{\text{aqu}}=0.471$  (II) was cooled down to 195 K, maintained there for 120 min. to ensure a complete ice recrystallization. Again, the existence of ‘liquid II phase of water’ seems to be mistakenly speculated basing on the behavior of the aqueous solutions falling in zone II.

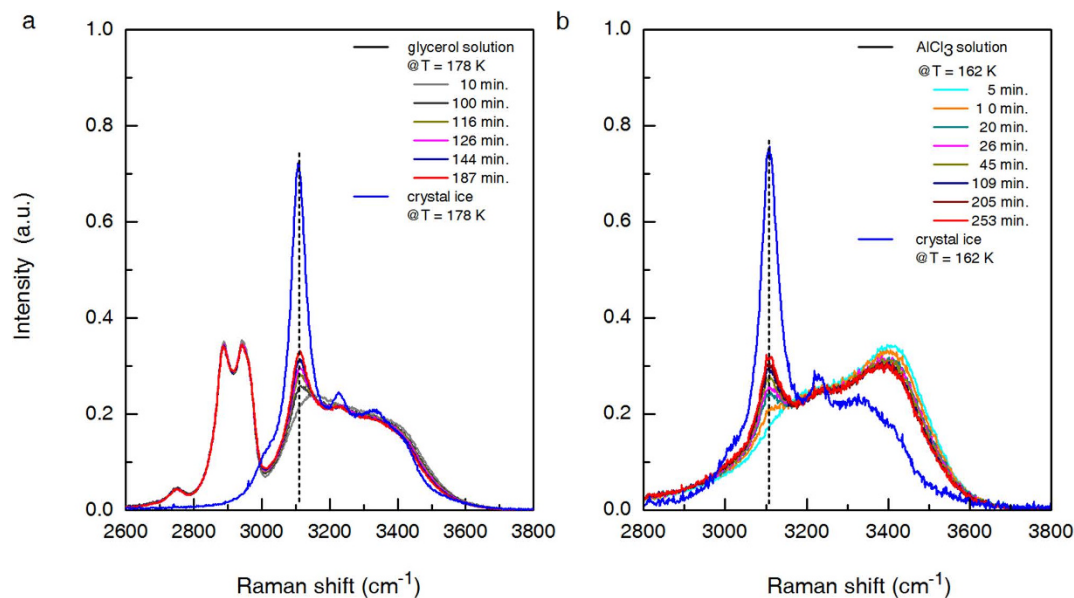


**Figure 3. Time-dependent Raman spectra of aqueous solutions in zone II of glycerol and  $\text{AlCl}_3$  under annealing treatment.** (a) Raman spectra for aqueous glycerol solution with  $X_{\text{aqu}} = 0.474$  maintained at  $T_a = 178$  K for a time interval up to 187 min. (b) The corresponding results for aqueous  $\text{AlCl}_3$  solution with  $X_{\text{aqu}} = 0.812$  annealed at 162 K for a time interval up to 253 min. For comparison, Raman spectra of ice Ih measured at the annealing temperatures are also presented.

**Raman spectrometric measurement.** The claimed LLT for water in aqueous solutions established on the measurement of glass transition temperature may probably arise from ice crystallization-induced phase separation, a point of view that has drawn attention from many researchers<sup>25,26</sup>. Authors of refs 18,19 also noticed the presence of ice in their annealed samples though, but they didn't think this is the reason for observed  $T_g$  shift. To exclude this possibility, time-dependent Raman spectra were also measured during annealing treatment<sup>18</sup>, and the shift from the high density liquid-like profile to the low density liquid-like profile, in the sample with a molar fraction of solute of 0.178 (i.e.,  $X_{\text{aqu}} = 0.474$  (II)) after annealing for 45 min. @171 K, was interpreted as a key evidence to the existence of LLT prior to ice recrystallization. Later, Suzuki and Mishima pointed out that it is inappropriate to compare the Raman spectra recorded at 171 K with those of the two kinds of amorphous ices recorded at 32 K<sup>17</sup>. We also traced the change in Raman spectra of glycerol solution with  $X_{\text{aqu}} = 0.474$  (II) annealed at  $T_a = 178$  K ( $< T_{\text{onset}}$ ) (Fig. 3a). After about 100 min., the OH-stretching band centered at  $\sim 3110$   $\text{cm}^{-1}$ , which is attributable to ice Ih, becomes obviously perceivable and gains intensity with increasing annealing time. In the case of aqueous  $\text{AlCl}_3$  solution with  $X_{\text{aqu}} = 0.812$  subject to annealing at 162 K (Fig. 3b), the OH-stretching band centered at  $\sim 3110$   $\text{cm}^{-1}$  already becomes perceivable after an annealing time of 10 min. All these observations point to the fact that for solutions falling in zone II, annealing at a temperature above glass-liquid transition temperature will effect ice recrystallization, and the subsequent measurement of a raised glass-liquid transition temperature is attributable to the freeze-concentration phase instead of a new phase of water.

In summary, by measuring the water-content dependence of glass transition temperature for various solutions in an as wide as possible concentration range, a universal feature characterized by two particular water contents,  $X_{\text{aqu}}^{\text{cr}}$ , above which a constant  $T_g'$  referring to the freeze-concentration phase is measured, and  $X_{\text{aqu}}'$  which corresponds to the freeze-concentration phase and refers to the hydration formula of the given solute, can be established. Solutions falling within zone II, i.e., with a water content  $X_{\text{aqu}}' < X_{\text{aqu}} < X_{\text{aqu}}^{\text{cr}}$ , can totally vitrify at a temperature  $T_g < T_g'$  under conventional one-round cooling/heating process at moderate rate, but annealing treatments at a temperature higher than the corresponding  $T_g$  can effectively evoke ice recrystallization, resulting in the measurement of a glass-liquid transition temperature  $T_g'$  which is obviously attributable to the freeze-concentrated phase. Experiments on aqueous solutions of glycerol and 1,2,4-butanetriol that were investigated in refs. 18 and 19 were carefully reproduced, and the samples were also subject to other annealing treatments to evoke ice recrystallization so as to reproduce the raised glass-liquid transition temperature which was interpreted as evidence for the existence of 'liquid II phase of water'. Together with dielectric relaxation and Raman spectroscopic measurements we can conclude unambiguously that the shift of glass-transition temperature by annealing treatment after vitrification/devitrification process is attributable to the freeze-concentrated phase of

solution instead of the ‘liquid II phase of water’, and the glass transition temperature of the so-called ‘liquid II phase of water’ is in fact the constant  $T_g'$  measured on all the solutions in zone I in which ice crystallization already occurs prior to the vitrification/devitrification. The disclosing of the universal water-content dependence of glass transition temperature is of essential importance in its own right, it provides a simple and reliable method to determine the hydration formula for solutes and to study the hydration behavior in mixture solutions.

## Methods

**Samples.** High-purity water was prepared by using a Millipore Milli-Q system. The solutes, purchased from Sigma-Aldrich, are  $ZnCl_2$  (anhydrous, 99.99%),  $AlCl_3 \cdot 6H_2O$  (99%), glycerol (99.5%), ethylene glycol (anhydrous, 99.8%), sorbitol (BioUltra,  $\geq 99.5\%$ ), and 1,2,4-butanetriol (98%).

**Differential scanning calorimetric measurement.** Measurement on droplets ( $\sim 5.0 \mu l$ ) of solutions was performed on a calorimeter (PE DSC8000) at a cooling/heating rate, unless specified, of  $20 K \text{ min}^{-1}$ . When cooled down to 113 K, the sample would be held at this temperature for 1 min. before the heating procedure began. Glass transition temperature was extracted from the devitrification peak on the heating curve. All the DSC curves have been normalized against sample weight. Details of the particular cooling/heating protocols designed for evoking ice recrystallization in a given solution are specified in text at proper places.

**Dielectric loss spectrometric measurement.** The dielectric spectra of samples, held in parallel plate sample cell BDS1308, were measured on a dielectric spectrometer (Novocontrol GmbH, Germany) equipped with a liquid nitrogen cooling system. The frequency ranges from 0.001 Hz to 10 MHz. For solutions falling within Zone II, each spectrum was measured when cooling the sample from room temperature down to the targeted temperature. After that, the sample was then heated up to room temperature so as to avoid ice recrystallization and to ensure that the measured spectra correspond to a single supercooled liquid solution. For solutions within Zone I and III and the annealed solutions within Zone II, temperature-dependent dielectric spectra were measured during heating the sample from 140 K up to room temperature.

**Raman spectrometric measurement.** Temperature-dependent Raman spectra were measured by using a Jobin-Yvon HR800 Raman system. For excitation, the spectral line at 532 nm of a laser was used. The temperature was adjusted by using a cooling unit (Linkam L-600 A) and a temperature controller (Linkam TMS 94).

## References

1. Poole, P. H., Sciortino, F., Essmann, U. & Stanley, H. E. Phase-Behavior of Metastable Water. *Nature* **360**, 324–328 (1992).
2. Harrington, S., Zhang, R., Poole, P. H., Sciortino, F. & Stanley, H. E. Liquid-liquid phase transition: Evidence from simulations. *Phys. Rev. Lett.* **78**, 2409–2412 (1997).
3. Palmer, J. C. *et al.* Metastable liquid-liquid transition in a molecular model of water. *Nature* **510**, 385–388 (2014).
4. Soper, A. K. & Ricci, M. A. Structures of high-density and low-density water. *Phys. Rev. Lett.* **84**, 2881–2884 (2000).
5. Mishima, O. & Stanley, H. E. The relationship between liquid, supercooled and glassy water. *Nature* **396**, 329–335 (1998).
6. Mishima, O. Reversible first-order transition between two  $H_2O$  amorphs at  $\sim 0.2$  Gpa and  $\sim 135$  K. *J. Chem. Phys.* **100**, 5910–5912 (1994).
7. Mishima, O. Liquid-liquid critical point in heavy water. *Phys. Rev. Lett.* **85**, 334–336 (2000).
8. Liu, L., Chen, S. H., Faraone, A., Yen, C. W. & Mou, C. Y. Pressure dependence of fragile-to-strong transition and a possible second critical point in supercooled confined water. *Phys. Rev. Lett.* **951**, 117802 (2005).
9. Mishima, O. Volume of supercooled water under pressure and the liquid-liquid critical point. *J. Chem. Phys.* **133**, 144503 (2010).
10. Holten, V. & Anisimov, M. A. Entropy-driven liquid-liquid separation in supercooled water. *Sci. Rep.* **2**, 713 (2012).
11. Mishima, O. & Stanley, H. E. Decompression-induced melting of ice IV and the liquid-liquid transition in water. *Nature* **392**, 164–168 (1998).
12. Limmer, D. T. & Chandler, D. The putative liquid-liquid transition is a liquid-solid transition in atomistic models of water. *J. Chem. Phys.* **135**, 134503 (2011).
13. Limmer, D. T. & Chandler, D. The putative liquid-liquid transition is a liquid-solid transition in atomistic models of water. II. *J. Chem. Phys.* **138**, 214504 (2013).
14. Angell, C. A. Formation of Glasses from Liquids and Biopolymers. *Science* **267**, 1924–1935 (1995).
15. Angell, C. A. Amorphous water. *Annu. Rev. Phys. Chem.* **55**, 559–583 (2004).
16. Kanno, H. & Angell, C. A. Homogeneous Nucleation and Glass Formation in Aqueous Alkali-Halide Solutions at High-Pressures. *J. Phys. Chem.* **81**, 2639–2643 (1977).
17. Suzuki, Y. & Mishima, O. Experimentally proven liquid-liquid critical point of dilute glycerol-water solution at 150 K. *J. Chem. Phys.* **141**, 094505 (2014).
18. Murata, K. I. & Tanaka, H. Liquid-liquid transition without macroscopic phase separation in a water-glycerol mixture. *Nat. Mater.* **11**, 436–443 (2012).
19. Murata, K. & Tanaka, H. General nature of liquid-liquid transition in aqueous organic solutions. *Nat. Commun.* **4**, 2844 (2013).
20. Mallamace, F. *et al.* Evidence of the existence of the low-density liquid phase in supercooled, confined water. *Proc. Nat. Acad. Sci. USA.* **104**, 424–428 (2007).
21. Zhang, Y. *et al.* Density hysteresis of heavy water confined in a nanoporous silica matrix, *Proc. Nat. Acad. Sci. USA.* **108**, 12206–12211 (2011).
22. Capaccioli, S., Ngai, K. L. & Shinyashiki, N. The Johari-Goldstein beta-relaxation of water. *J. Phys. Chem. B* **111**, 8197–8209 (2007).

23. Grzybowska, K., Grzybowski, A., Pawlus, S., Hensel-Bielowka, S. & Paluch, M. Dielectric relaxation processes in water mixtures of tripropylene glycol. *J. Chem. Phys.* **123**, 204506 (2005).
24. Leon, C., Ngai, K. L. & Roland, C. M. Relationship between the primary and secondary dielectric relaxation processes in propylene glycol and its oligomers. *J. Chem. Phys.* **110**, 11585–11591 (1999).
25. Hayashi, Y., Puzenko, A. & Feldman, Y. Ice nanocrystals in glycerol-water mixtures. *J. Phys. Chem. B* **109**, 16979–16981 (2005).
26. Limmer, D. T. & Chandler, D. Corresponding states for mesostructure and dynamics of supercooled water. *Faraday Discuss.* **167**, 485–498 (2013).

### Acknowledgements

This work was supported by NSFC grant nos. 11290161, 51172272 and 11474325, by the Chinese Academy of Sciences grant no.KJZD-EW-M03, and by the National Basic Research Program of China grant no. 2010CB630705.

### Author Contributions

Q.W. initiated the research, L.S.Z. and Q.W. performed the measurement, Q.W. and Z.X.C. interpreted the result, Q.W. and Z.X.C. compiled the manuscript.

### Additional Information

**Supplementary information** accompanies this paper at <http://www.nature.com/srep>

**Competing financial interests:** The authors declare no competing financial interests.

**How to cite this article:** Zhao, L.-S. *et al.* Glass transition of aqueous solutions involving annealing-induced ice recrystallization resolves liquid-liquid transition puzzle of water. *Sci. Rep.* **5**, 15714; doi: 10.1038/srep15714 (2015).



This work is licensed under a Creative Commons Attribution 4.0 International License. The images or other third party material in this article are included in the article's Creative Commons license, unless indicated otherwise in the credit line; if the material is not included under the Creative Commons license, users will need to obtain permission from the license holder to reproduce the material. To view a copy of this license, visit <http://creativecommons.org/licenses/by/4.0/>